

Phase Transfer Catalysts Drive Diverse Organic Solvent Solubility of Single-Walled Carbon Nanotubes Helically Wrapped by Ionic, Semiconducting Polymers

Pravas Deria,[†] Louise E. Sinks,^{‡,||} Tae-Hong Park,[‡] Diana M. Tomezsko,[‡] Matthew J. Brukman,[§] Dawn A. Bonnell,[§] and Michael J. Therien ^{*,†}

[†]Department of Chemistry, French Family Science Center, 124 Science Drive, Duke University, Durham,

North Carolina 27708, [‡]Department of Chemistry, University of Pennsylvania, 231 South 34th Street, Philadelphia, Pennsylvania 19104, and [§]Department of Materials Science and Engineering, University of Pennsylvania, 3231 Walnut Street, Philadelphia, Pennsylvania 19104

ABSTRACT Use of phase transfer catalysts such as 18-crown-6 enables ionic, linear conjugated poly[2,6-{1,5-bis(3-propoxy-sulfonic acidsodiumsalt)}naphthylene]ethynylene (PNES) to efficiently disperse single-walled carbon nanotubes (SWNTs) in multiple organic solvents under standard ultrasonication methods. Steady-state electronic absorption spectroscopy, atomic force microscopy (AFM), and transmission electron microscopy (TEM) reveal that these SWNT suspensions are composed almost exclusively of individualized tubes. High-resolution TEM and AFM data show that the interaction of PNES with SWNTs in both protic and aprotic organic solvents provides a self-assembled superstructure in which a PNES monolayer helically wraps the nanotube surface with periodic and constant morphology (observed helical pitch length = 10 ± 2 nm); time-dependent examination of these suspensions indicates that these structures persist in solution over periods that span at least several months. Pump–probe transient absorption spectroscopy reveals that the excited state lifetimes and exciton binding energies of these well-defined nanotube-semiconducting polymer hybrid structures remain unchanged relative to analogous benchmark data acquired previously for standard sodium dodecylsulfate (SDS)-SWNT suspensions, regardless of solvent. These results demonstrate that the use of phase transfer catalysts with ionic semiconducting polymers that helically wrap SWNTs provide well-defined structures that solubilize SWNTs in a wide range of organic solvents while preserving critical nanotube semiconducting and conducting properties.

KEYWORDS Single chain, helical wrapping, ionic poly(aryleneethynylene), phase transfer catalyst, SWNTs, organic solvent

Single wall carbon nanotubes (SWNTs)^{1–4} possess a wide range of uncommon mechanical,^{5–9} optical,^{1,10–12} electrical,^{13–17} magnetic,^{18–21} and thermal^{22,23} properties that fuel multidisciplinary efforts aimed at developing neoteric nanoscale, microscale, and bulk-phase materials.² Strong van der Waals interactions between SWNTs^{24,25} are an anathema to SWNT solubilization.¹³ Water-solubilized SWNTs dominate the literature; there exists no general method to disperse SWNTs in nonaqueous media. Potential dispersion approaches are truncated severely by the fact that preservation of significant SWNT electrooptic properties require solubilization via agents that noncovalently interact with the nanotube surface.^{24,25} It has thus been a long-standing goal to develop a universal SWNT solubilization strategy that (i) relies on noncovalent interactions for nanotube dispersion, (ii) provides a high yield of

individualized tubes, (iii) enables dispersion in a wide range of dielectric media, and yet (iv) gives rise to suspended SWNT structures having a constant morphology, regardless of solvent.

Ultrasonication^{11,26} and high-speed vibrational milling techniques²⁷ are commonly utilized to drive exfoliation of nanotube ropes and bundles in the presence of surfactants, small molecules, and polymers.²⁸ The huge library of established noncovalent nanotube solubilizing agents is dominated by species that only exfoliate tubes in an aqueous medium; surfactants such as SDS,¹¹ SDBS,^{29,30} and sodium cholate,³¹ and amphiphilic aromatic molecules,³² typify these SWNT-solubilizing compositions. Flexible polymers such as polystyrene sulfonate (PSS), polyvinyl pyrrolidone (and their poly acrylic and maleic acid-containing copolymers),³³ α -helical amphiphilic peptides,³⁴ DNA,^{35–37} sodium carboxymethylcellulose (Na-CMC),³⁸ and β -1,3-glucans³⁹ also wrap SWNTs in water. Among these agents, only β -1,3-glucans and DNA wrap individualized SWNTs with a fixed periodicity; notably, neither of these biological polymers disperse SWNTs in organic solvent to provide well-defined structures of similar morphology. Further, multiple studies

* To whom correspondence should be addressed. Tel: 919-660-1670. Fax: 919-660-1605. E-mail: michael.therien@duke.edu.

|| Present address: Department of Biochemistry and Biophysics, University of Pennsylvania, 317 Anatomy-Chemistry Bldg., 36th Street and Hamilton Walk, Philadelphia, PA 19104.

Received for review: 07/20/2010

Published on Web: 09/01/2010

show that transferring SWNTs wrapped with an amphiphilic polymer from an aqueous to an organic phase results in polymer dewrapping and SWNT precipitation.^{33,39} Finally, hydrophobic conjugated polymers based on PmPV,⁴⁰ poly-thiophene,²⁷ polyfluorene,⁴¹ and poly(*p*-phenyleneethynylene)⁴² frameworks can disperse SWNTs in variety of nonaqueous solvents, but all such structurally characterized SWNT samples display microscopy consistent with indistinct rod structures and substantial polymer/SWNT molar ratios; a classic example of this can be seen in work by Smalley,³³ which shows that flexible polymers wrap SWNTs with very short pitch lengths that give rise to thick polymer-SWNT hybrid structures indicative of multiple polymer chains associated per SWNT.

We have reported that poly[*p*-{2,5-bis(3-propoxysulfonic acid sodium salt)}phenylene]ethynylene (PPES), a linear conjugated polymer, disentangles SWNT strands from their bundled forms at high mass percent conversion in water; interestingly, in contrast to previous studies in which other *p*-phenyleneethynylene-based polymers have been shown to interact with SWNTs in a parallel fashion,⁴² PPES wraps SWNTs forming a single-stranded, self-assembled helical super structure having a well-defined pitch length of 13 ± 2 nm.⁴³ Here we show that phase transfer catalysts, used in combination with the highly charged semiconducting poly[2,6-{1,5-bis(3-propoxysulfonic acidsodiumsalt)}naphthylene]ethynylene (PNES), provides individualized SWNTs that are soluble in a wide-range of organic solvents. Notably, the morphology and electronic structure of these constructs remain uniform, regardless of the solvent dielectric.

Experimental Methods. PNES was synthesized via the Suzuki–Miyaura polycondensation reaction^{44–47} of 1,2-bis(4',4',5',5'-tetramethyl[1',3',2']dioxaborolan-2'-yl)ethyne⁴⁴ and {[2,6-diiodo-1,5-bis(3-propoxysulfonic acid)sodium salt]}. The M_n of PNES was determined to be ~ 18.8 kD via anion exchange chromatography, which corresponds to a degree of polymerization (DP) of ~ 40 and a PDI of 1.11 (Supporting Information Figure S2). SWNTs were suspended in various solvents using the standard ultrasonication-centrifugation technique.^{11,43} A 2.5 mL solution of ionic PNES (1.68 mg/mL) was sonicated with 2 mg of HipCo (batch 81) nanotubes in direct contact with a tip horn sonicator (20 kHz), and centrifuged (36000 g; 3 h). The upper 60% of the supernatant was collected. The preparation of an aqueous suspension involves SWNT prewetting with 0.1 mL DMF and sonication for 3 h (1 W/mL). Organic suspensions were obtained by dissolving PNES in the desired solvent with the phase transfer catalyst 18-crown-6 (~ 20 mg/mL); sonication conditions: 0.5–1 h; 0.4 W/mL. SDS-SWNT suspensions in water were prepared using a literature process.⁴³ Transmission electron microscopy images (JEOL TEM-2010; accelerate voltage, 80 kV) were obtained from samples prepared via drop casting on lacy Formvar copper grids stabilized with carbon followed by drying in a desiccator. Atomic force microscopy (AFM; Digital Instruments Dimension 3100)

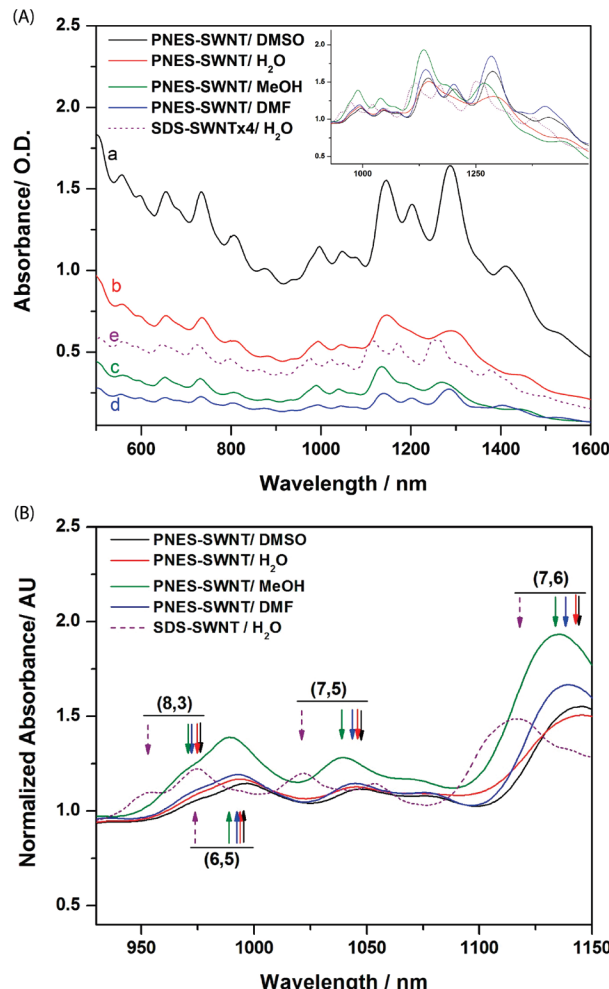
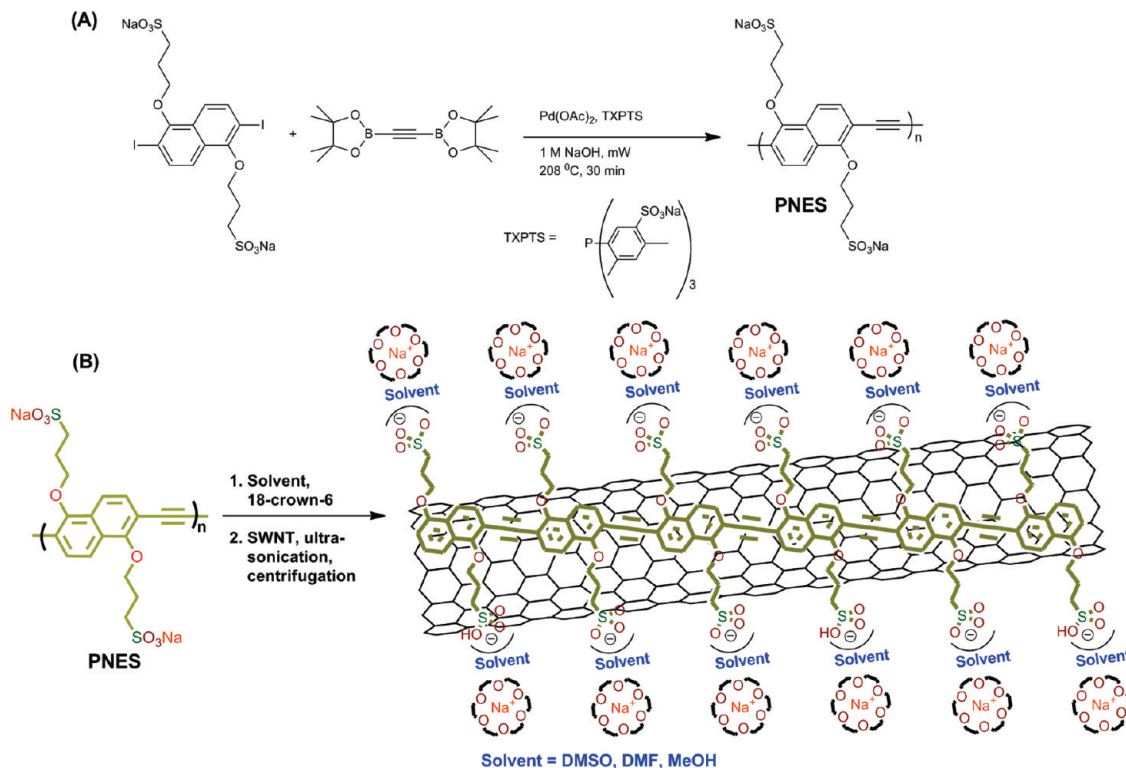


FIGURE 1. (A) Solvent-dependent vis-NIR absorption spectra of PNES-SWNTs and SDS-SWNT samples. PNES-SWNT suspensions: (a) DMSO (black), (b) H₂O (red), (c) MeOH (green), and (d) DMF (blue); the dashed spectrum (e) corresponds to that for the aqueous SDS-SWNT benchmark (purple), which is shown scaled by a factor of 4. Optical path length = 1 mm. Inset: spectra normalized at 910 nm for comparative purposes showing the solvent-dependent spectral evolution of long-wavelength PNES-SWNT transitions relative to those for the SDS-SWNT benchmark. (B) NIR absorption spectra, normalized at 910 nm, of PNES-SWNT samples suspended in DMSO (black), H₂O (red), MeOH (green), and DMF (blue) solvents; the dashed spectrum corresponds to that for the aqueous SDS-SWNT benchmark (purple). The relative peak positions of the prominent absorption maxima assigned to (6,5), (8,3), (7,5) and (7,6) SWNTs are marked with arrows, highlighting the extent of solvent-dependent spectral red shifts of these transitions for PNES-SWNT suspensions in organic solvents, relative to the respective absorption maxima observed for the SDS-SWNT benchmark.

images were obtained via intermittent contact mode (scan rate = 2 Hz, Si tip, ambient temperature). AFM samples were prepared by drop-casting SWNT suspensions on Si wafer or freshly cleaved mica surfaces; such samples were then desiccator-dried for 30 min. Electronic spectra were recorded on a Varian 5000 UV-vis/NIR instrument. The relative peak positions (Figure 1b) were assigned via spectral deconvolution using Origin 7.5 software. Excited state dynamical studies were performed using a femtosecond spectroscopy

SCHEME 1. (A) Synthesis of the Highly Charged Polymer, PNES, from {[2,6-Diiodo-1,5-bis(3-propoxysulfonicacid)naphthalene] sodium salt} and (B) Depiction of Phase Transfer Catalyst-Mediated Dispersion of PNES-SWNTs in Organic Solvents



system.⁴⁸ Samples were interrogated in 2 mm path-length fused-silica cells under argon.

A more detailed description of these experimental methods can be found in Supporting Information.

Result and Discussion. It has been well established that meta-bridged aryleneethynylene foldamers provide flexible helical structures where the interior pore size and other metrical parameters evolve as a function of chain length, solvent, and temperature.^{49,50} Less, however, is known regarding the helix-forming propensities of related aryleneethynlenes having a para linkage topology. Computational data indicated that the binding energy difference between potential parallel and optimal helical PPES/SWNT conformations is ~ 1.1 kcal/mol/monomer and underscored that the total energy stabilized via the polymer helical wrapping interaction accumulates as the number of unit monomers increases.⁴³ Given the larger aromatic surface area of naphthalene relative to phenylene, and the fact that the 2,6-aryleneethynylene linkage topology of PNES should drive a smaller polymer-SWNT helical pitch relative to that determined previously for 1,4-phenyleneethynylene-linked PPES, PNES-wrapped SWNT structures would be anticipated to display augmented thermodynamic stability. PNES was synthesized from 1,2-bis(4',4',5',5'-tetramethyl-[1',3',2']dioxaborolan-2'-yl)ethyne and {[2,6-diiodo-1,5-bis(3-propoxysulfonicacid)naphthalene] sodium salt} via the Suzuki–Miyaura polycondensation reaction⁴⁴ in water (Scheme 1a; Supporting Information).

Polyanionic PNES (see Supporting Information for polymer characterization data) disperses readily SWNTs (HipCo tubes batch 81) into the aqueous phase. The dissolved SWNT mass was estimated by examination of the integrated electronic absorption oscillator strength over a 600 to 1600 nm wavelength range, referenced to established literature benchmarks, where the oscillator strength of a maximally concentrated sodium dodecylsulfate (SDS) suspended SWNT sample (SDS-SWNT) was taken to be 1.^{29,35,38,43,51} SWNT mass dispersion in water reaches a maximum (~ 0.37 mg/mL) at ~ 3 h of sonication time regardless of sonication power (0.4–4 W/mL; Supporting Information).⁴³

Phase transfer catalysts, which facilitate movement of a reactant from an aqueous phase to organic medium, have had tremendous impact in the field of organic synthesis; these agents accelerate reaction rates, make possible heterogeneous chemical reactions, and minimize solvent waste.⁵² PNES is insoluble in all common organic solvents. Addition of the phase transfer catalyst 1,4,7,10,13,16-hexaoxacyclooctadecane (18-crown-6) to organic solvents enables PNES Na^+ complexation and solvation and polymer dissolution. Sonication of SWNTs in such PNES organic solvent solutions made possible via the use of phase transfer catalysts, drives nanotube dispersion; well-established sonication-centrifugation methods^{11,43,48} enable isolation of PNES-solubilized SWNTs (Scheme 1b) in organic media.

TABLE 1. NIR Electronic Absorption Band Maxima for PNES-Wrapped (6,5), (8,3), (7,5), and (7,6) SWNTs, As a Function of Solvent, Relative to the Analogous Electronic Transitions Observed for the SDS-SWNT Benchmark in Water

system ^a (ϵ , solvent) ^b	(6,5)		(8,3)		(7,5)		(7,6)	
	E11 (nm)	shift ^c (cm ⁻¹)	E11 (nm)	shift ^c (cm ⁻¹)	E11 (nm)	shift ^c (cm ⁻¹)	E11 (nm)	shift ^c (cm ⁻¹)
SDS H ₂ O (80)	975		954		1022		1120	
PNES H ₂ O (80)	994	196	974	215	1045	215	1146	202
PNES DMSO (47)	996	216	970	172	1046	224	1146	202
PNES MeOH (33)	989	145	967	141	1040	169	1135	118
PNES DMF (38)	992	176	972	194	1045	215	1138	141

^a Surfactant/solvent system. ^b Solvent bulk dielectric constant. ^c Spectral red shift relative to that for the analogous transition observed for the aqueous SDS-SWNT benchmark.

Sonication times to achieve maximal SWNT mass dispersion varied as a function of solvent (DMSO, DMF, CH₃OH), but were considerably shorter (0.5–1 h) than that required to prepare concentrated aqueous solutions, with dispersed SWNT masses ranging from 0.14 (DMF) to 0.64 mg/mL (DMSO). Steady state vis-NIR absorption spectra (Figure 1a) highlight the relative maximal, PNES-dispersed SWNT masses as a function of solvent relative to that determined for the SDS-SWNT benchmark in water. Note that sharp spectral transitions, similar to that observed for the SDS-SWNT reference spectrum (Figure 1), suggest that in these organic solvents, interaction with PNES drives fully exfoliated SWNT suspensions consisting largely of individualized tubes (vide infra). The prominent first and second subband absorption manifolds of these PNES-SWNT suspensions exhibit marked spectral red shifts, and modest absorption band broadening, relative to the SDS-SWNT benchmark spectrum. Figure 1b displays absorptions assigned previously to (6,5), (8,3), (7,5), and (7,6) nanotubes^{1,53} and highlights the extent of the spectral red shifts in PNES-SWNT suspensions for these bands with respect to the corresponding reference transitions in the SDS-SWNT spectrum. Table 1 shows that while the degree of these PNES-SWNT transition red shifts range from 115 to 225 cm⁻¹, the absolute shift magnitude depends clearly on both tube chirality and solvent [MeOH ($\epsilon = 33$; 118–170 cm⁻¹) < DMF ($\epsilon = 38$; 141–215 cm⁻¹) < H₂O ($\epsilon = 80$; 196–215 cm⁻¹) ~DMSO ($\epsilon = 47$; 172–224 cm⁻¹)]; these spectral dependences are notably consistent with the theoretical predictions made by Strano and Choi which have heretofore lacked experimental precedent.⁵⁴ These data thus suggest that whereas the PNES-SWNT π – π interaction is a primary driving force for the observed transition spectral shifts relative to the SDS-SWNT aqueous benchmark,^{11,43,55} the solvent-dependent local dielectric environment plays a significant role in determining PNES-SWNT electronic spectral properties.⁵⁴

High-resolution transmission electron microscopy (TEM) and atomic force microscopy (AFM) experiments (Figures 2–3; Supporting Information Figures S6–7) that interrogate PNES-SWNT structures formed in H₂O, CH₃OH, DMF, and DMSO reveal that all of these samples are composed overwhelmingly of individualized nanotubes (80–90 %) that are periodically wrapped by single strands of this highly charged aryleneethynylene polymer. Remarkably, these data show

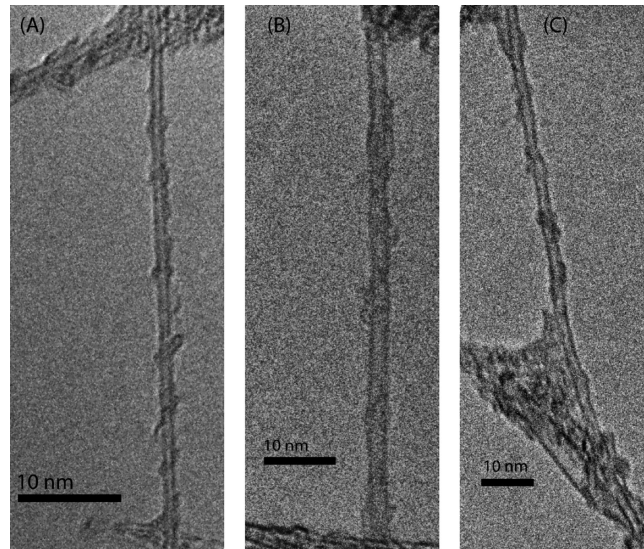


FIGURE 2. TEM images of PNES-wrapped SWNTs obtained from (A) aqueous, (B) DMSO, and (C) DMF suspensions. (See Supporting Information for sample preparations).

that PNES-SWNT structures maintain constant morphology regardless of solvent. As observed for PPES-SWNT compositions formed in aqueous media,⁴³ PNES-SWNTs manifest regular, helically wrapped structures. TEM images of PNES-SWNTs (Figure 2; Supporting Information Figures S12, S16, and S17) show small, repeating protuberances at 9–11 nm intervals along the SWNT axis with an ~3 nm lateral shift which remains invariant in aqueous, CH₃OH, DMF, and DMSO solvents. As anticipated, this observed PNES helical pitch length of ~10 nm is diminished with respect to that observed for PPES-SWNTs (~13 nm). This observed repeating structural signature for helical wrapping by PNES is also evidenced for two-tube bundles (Supporting Information Figures S13–14), where the observed helical pitch is shorter (~7 ± 2 nm) than that obtained for individualized tubes, confirming that helical pitch length systematically tracks with bundle size. Likewise, AFM images of PNES-SWNTs dispersed in water, DMF, DMSO, and MeOH, along with corresponding height profile analyses (Figure 3), corroborate the PNES-SWNT helical wrapping evident in the TEM data. Note also that the periodic wavelike height profiles apparent in these microscopy experiments parallel related images that verify helical wrapping of SWNTs by polymers.^{39,43} Ad-

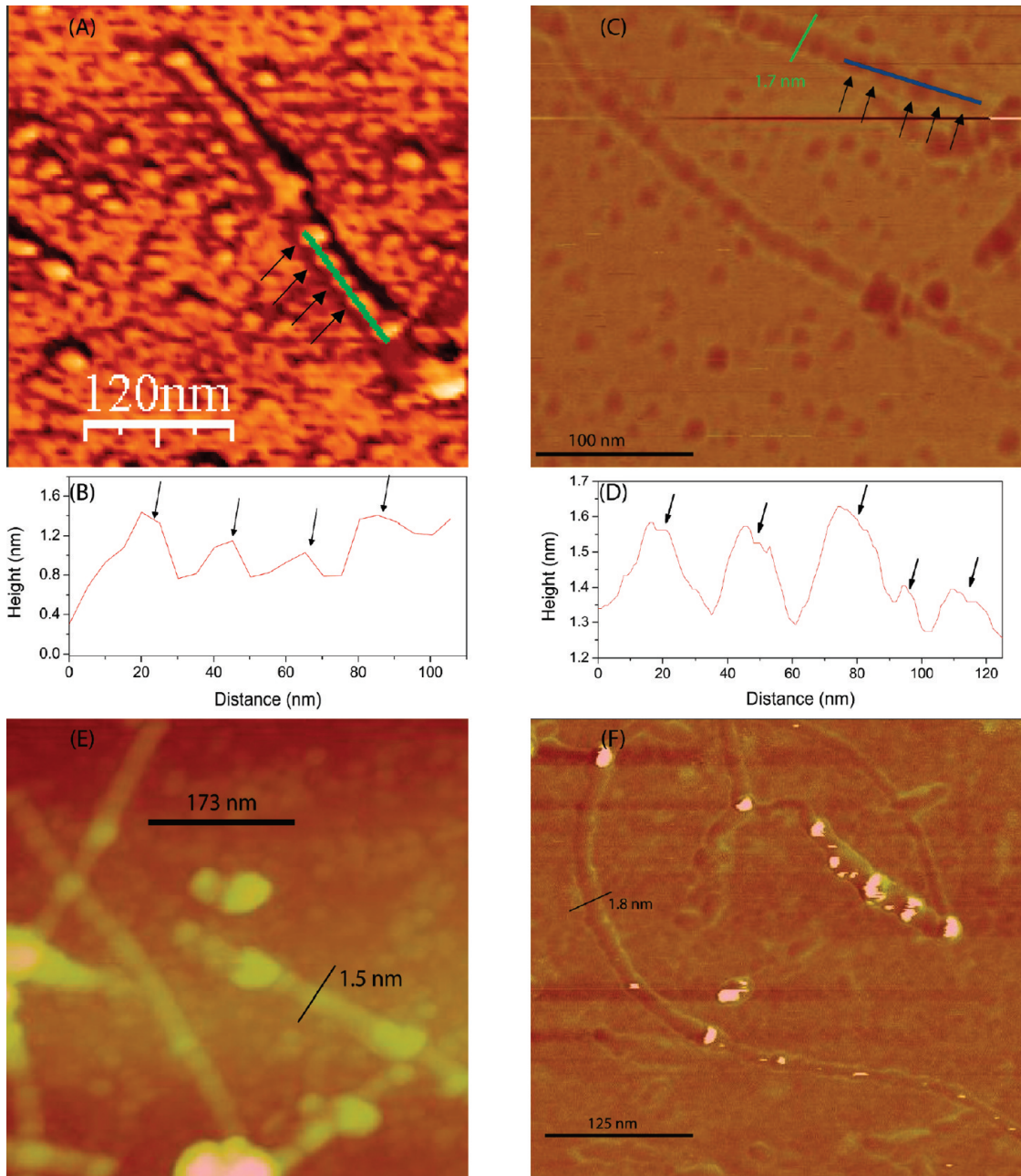


FIGURE 3. Topographic intermittent contact mode AFM images of PNES-SWNTs. (A) PNES-SWNTs from a H₂O-solubilized suspension on a Si surface; (B) corresponding height profile along the green line in the panel (A) data; (C) PNES-SWNTs from a DMF-solubilized suspension on a mica surface; (D) corresponding height profile along the blue line of the panel (C) data; (E,F) PNES-SWNTs from DMSO and MeOH-solubilized suspensions respectively on mica surfaces; the thicknesses of these single-strand, PNES-wrapped SWNTs are indicated in the panel (C), (E) and (F) data.

ditional electronic absorption and AFM data (Supporting Information) highlight that PNES-SWNT morphology, and the extent to which SWNTs are individualized, remain unchanged over time periods ranging from several months to one year, regardless of the solvent suspension medium. EDS and XPS experiments that interrogate elemental composition corroborate single chain helical wrapping of the SWNT surface by PNES (Supporting Information Figures S18–21).

To provide additional insight into the extent to which PNES helical wrapping impacts SWNT electronic structural properties, ultrafast pump–probe spectroscopy was employed to interrogate the electronically excited states of these species and their corresponding transient dynamics as a function of solvent. Exciting an aqueous suspension of HipCo (batch 81) SWNTs at 775 nm (4 μ J/pulse pump power) and probing in the second subband region (Figure 4), evinced similar excited state dynamics as that reported previously for

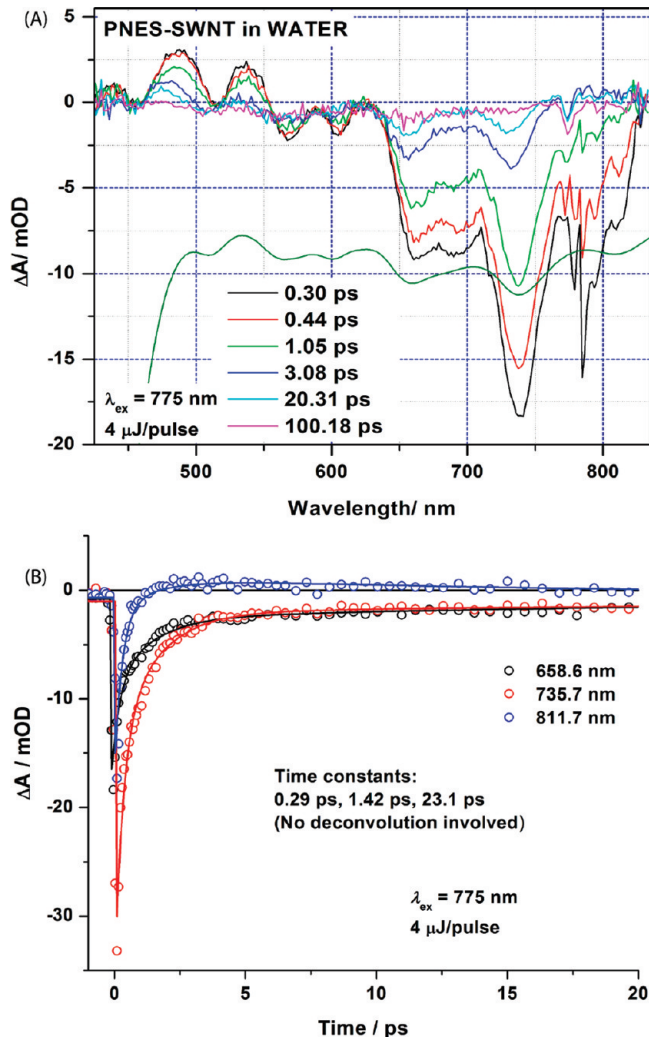


FIGURE 4. (A) Transient absorption spectra of a PNES-SWNT sample in water with labeled delay times determined under ambient conditions at magic angle polarization ($\lambda_{\text{ex}} = 775 \text{ nm}$; 4 $\mu\text{J}/\text{pulse}$). An inverted, scaled PNES-SWNT linear absorption spectrum is shown for comparison. (B) Representative transient decay kinetics obtained for aqueous PNES-SWNT suspensions. The best triexponential function global fits for these data are depicted by thin lines. The evaluated characteristic decay time constants for these transient decay profiles are shown as an inset.

analogous SDS-SWNTs in water.^{48,56} A triexponential function global fit of the transient kinetics at 658, 736, and 812 nm (Figure 4b) indicates SWNT excited-state lifetime time constants of 0.29, 1.42, and 23.1 ps, which have respectively been ascribed previously to intraband carrier relaxation, intertube energy transfer, and inherent lowest excited state relaxation processes in the SDS-SWNT benchmark.^{48,56} These data demonstrate that SWNT excited-state relaxation dynamics are not perturbed by the strong $\pi-\pi$ interactions that help drive helical PNES wrapping of the SWNT surface.

It is known that the optical resonances in SWNTs are excitonic,^{12,57} and that the exciton binding energy of semiconducting SWNTs constitutes a substantial amount of the total band gap energy. Given the nature of the PNES-SWNT

interaction, and the fact that the exciton binding energy can depend intimately on the local dielectric environment, we investigated the exciton binding energies of PNES-SWNTs in a wide range of dielectric media; Figure 5 summarizes these data. PNES-SWNT samples were excited at 670 nm, a wavelength known to produce an excited state population dominated by (8,3) tubes, at various pump intensities; in these experiments, a bleach band centered at $\sim 735 \text{ nm}$ was observed for PNES-SWNT samples suspended in H₂O, DMSO, DMF, and MeOH (Figure 5a). These data were analyzed using an approach described previously by Fleming,⁵⁸ where the (8,3) tube exciton binding energy ($\sim 0.41 \text{ eV}$) was determined from the energy difference between the electron–hole (e–h) continuum and its precursor exciton. Similar to data acquired for SDS-SWNTs,⁵⁸ the 735 nm transient signal observed for PNES-SWNTs (Figure 5b,c) linearly follows e–h continuum kinetics $[n_{\text{eh}}(0)/n_{\text{eh}}(t)]^2 - 1 = \gamma_A n_{\text{eh}}^2(0)t$, regardless of solvent, and not annihilation kinetics $[n_{\text{ex}}(0)/n_{\text{ex}}(t)] - 1 = \gamma_{\text{ex}} n_{\text{ex}}(0)t$ (γ_A and γ_{ex} are the rate constants of the respective nonlinear relaxation process, and $n_{\text{ex}}(t)$ and $n_{\text{eh}}(t)$ are the populations of excitons and charged carriers).⁵⁹ Data summarized in Figure 5d,e show that transient kinetics probed at 735 nm are independent of E_2 pump intensity at 670 nm, indicating that exciton dissociation occurs from the E₁ exciton precursor. Confirming the identity of the $\sim 735 \text{ nm}$ peak as an e–h continuum band (E_{eh}), the respective exciton binding energies (E_b) calculated from E_{eh} and E₁ determined in H₂O, DMSO, MeOH, and DMF solvents were found to be 0.414, 0.409, 0.405, and 0.411 eV. These values, which are of similar magnitude to literature benchmarks,^{12,58,60,61} show that there is no substantial perturbation to SWNT exciton binding energies due to conjugated polymer wrapping and use of phase-transfer reagents, and suggest that the small differences in these measured E_b values derive from local environmental dielectric disparities.

Conclusions. This work shows that the phase transfer catalyst 18-crown-6 enables ionic poly[2,6-{1,5-bis(3-propoxysulfonic acidsodiumsalt)}naphthylene]ethynylene (PNES) to exfoliate and individualize SWNTs in organic solvents. AFM and TEM data of these organic-solvent-suspended SWNTs demonstrate that the PNES-SWNT interaction provides a self-assembled superstructure in which a PNES monolayer helically wraps the nanotube surface with periodic and constant morphology (helix pitch length = 10 $\pm 2 \text{ nm}$); such monolayer wrapping minimizes the polymer/SWNT molar ratio of the organic-solvent soluble SWNT composition. In contrast to other work that has examined SWNTs enveloped by amphiphilic polymers, these PNES-SWNTs do not exhibit polymer dewrapping and SWNT precipitation in organic solvents; DMSO-, DMF-, and MeOH-solubilized SWNTs have been shown to persist in solution over time periods that exceed at least several months. Steady-state and time-resolved transient optical spectroscopic studies indicate that PNES-SWNTs of a given nanotube chirality retain electronic structural homogeneity re-

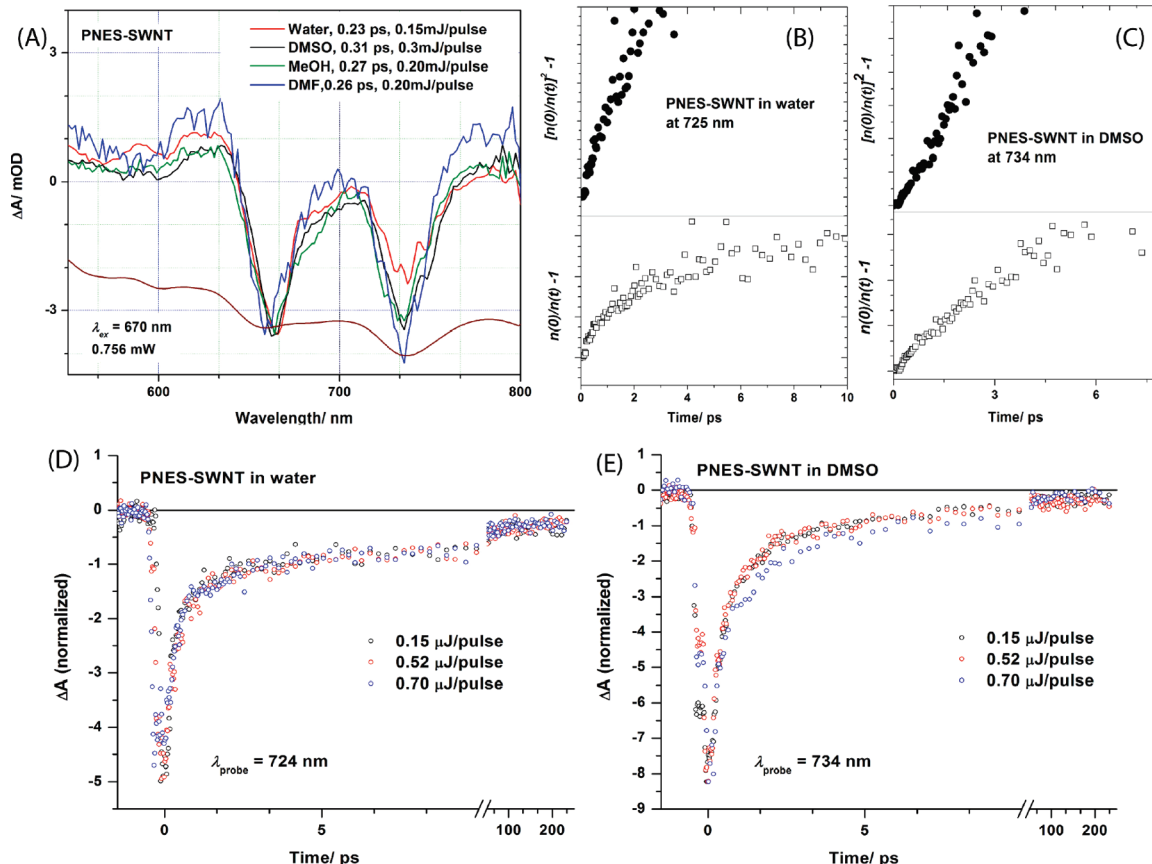


FIGURE 5. (A) Transient absorption spectra of PNES-SWNT samples in water (red), DMSO (black), MeOH (green), and DMF (blue), normalized at 660 nm, with labeled delay times and pump energies, determined at magic angle polarization ($\lambda_{\text{ex}} = 670 \text{ nm}$). An inverted, scaled PNES-SWNT linear absorption spectrum in water is shown for comparison. (B) Plot of $([\ln(0)/\ln(t)] - 1)$ and $([\ln(0)/\ln(t)]^2 - 1)$ vs time obtained for a PNES-SWNT suspension in water recorded at 725 nm at a 0.15 mJ/pulse pump fluence. (C) Plot of $([\ln(0)/\ln(t)] - 1)$ and $([\ln(0)/\ln(t)]^2 - 1)$ vs time for a PNES-SWNT suspension in DMSO solvent recorded at 734 nm at a 0.30 mJ/pulse pump fluence. (D) Normalized kinetics probed at 725 nm for a range of pump intensities for an aqueous PNES-SWNT suspension. (E) Normalized kinetics probed at 734 nm for a range of pump intensities for a PNES-SWNT sample suspended in DMSO solvent.

gardless of solvent. Conjugated, highly charged semiconducting polymers, used in combination with a suitable phase transfer agent, thus provide a general means to deliver individualized, noncovalently modified SWNTs of fixed morphology that retain established nanotube semiconducting and conducting properties in a wide range of dielectric media.

Acknowledgment. This work was supported by a grant from the Office of Naval Research (N00014-06-1-0360). The authors thank the United States Department of Energy (EFRC-P353-0127), as well as the MRSEC (DMR-00-79909) and NSEC (DMR-0425780) programs of the National Science Foundation for infrastructural support. M.J.T. is grateful to the Francqui Foundation (Belgium), and VLAC (Vlaams Academisch Centrum), Centre for Advanced Studies of the Royal Flemish Academy of Belgium for Science and the Arts for research fellowships. We thank Dr. Amar Kumbhar and Dr. Carrie Donley at Chapel Hill Analytical and Nanofabrication Laboratory (CHANL) at University of North Carolina, Chapel Hill for performing the SEM/EDS and XPS experiments.

Supporting Information Available. PNES-SWNT preparative procedures, TEM and AFM experimental details, additional spectroscopic, microscopy, and elemental analysis data. This material is available free of charge via the Internet at <http://pubs.acs.org>.

REFERENCES AND NOTES

- Bachilo, S. M.; Strano, M. S.; Kittrell, C.; Hauge, R. H.; Smalley, R. E.; Weisman, R. B. *Science* **2002**, *298*, 2361–2366.
- Dresselhaus, M.; Dresselhaus, G.; Avouris, P. *Carbon Nanotubes: Synthesis, Properties, and Applications*; Springer-Verlag: Berlin, 2001.
- Iijima, S.; Ichihashi, T. *Nature* **1993**, *363*, 603–605.
- Bethune, D. S.; Kiang, C. H.; de Vries, M. S.; Gorman, G.; Savoy, R.; Vazquez, J.; Beyers, R. *Nature* **1993**, *363*, 605–607.
- Baughman, R. H.; Cui, C.; Zakhidov, A. A.; Iqbal, Z.; Barisci, J. N.; Spinks, G. M.; Wallace, G. G.; Mazzoldi, A.; De Rossi, D.; Rinzler, A. G.; Jaschinski, O.; Roth, S.; Kertesz, M. *Science* **1999**, *284*, 1340–1344.
- Kim, P.; Lieber, C. M. *Science* **1999**, *286*, 2148–2150.
- Yu, M.-F.; Files, B. S.; Arepalli, S.; Ruoff, R. S. *Phys. Rev. Lett.* **2000**, *84*, 5552–5555.
- Ajayan, P. M.; Stephan, O.; Colliex, C.; Trauth, D. *Science* **1994**, *265*, 1212–1214.

- (9) Tombler, T. W.; Zhou, C.; Alexseyev, L.; Kong, J.; Dai, H. J.; Liu, L.; Jayanthi, C. S.; Tang, M.; Wu, S.-Y. *Nature* **2000**, *405*, 769–772.
- (10) Misewich, J. A.; Martel, R.; Avouris, P.; Tsang, J. C.; Heinze, S.; Tersoff, J. *Science* **2003**, *300*, 783–786.
- (11) O'Connell, M. J.; Bachilo, S. M.; Huffman, C. B.; Moore, V. C.; Strano, M. S.; Haroz, E. H.; Rialon, K. L.; Boul, P. J.; Noon, W. H.; Kittrell, C.; Ma, J.; Hauge, R. H.; Weisman, R. B.; Smalley, R. E. *Science* **2002**, *297*, 593–596.
- (12) Wang, F.; Dukovic, G.; Brus, L. E.; Heinz, T. F. *Science* **2005**, *308*, 838–841.
- (13) Baughman, R. H.; Zakhidov, A. A.; de Heer, W. A. *Science* **2002**, *297*, 787–792.
- (14) Bockrath, M.; Cobden, D. H.; McEuen, P. L.; Chopra, N. G.; Zettl, A.; Thess, A.; Smalley, R. E. *Science* **1997**, *275*, 1922–1925.
- (15) Dai, H.; Wong, E. W.; Lieber, C. M. *Science* **1996**, *272*, 523–526.
- (16) Tans, S. J.; Verschueren, A. R. M.; Dekker, C. *Nature* **1998**, *393*, 49–52.
- (17) Liang, W.; Bockrath, M.; Bozovic, D.; Hafner, J. H.; Tinkham, M.; Park, H. *Nature* **2001**, *411*, 665–669.
- (18) Man, H. T.; Morpurgo, A. F. *Phys. Rev. Lett.* **2005**, *95*, No. 026801–026804.
- (19) Zaric, S.; Ostojic, G. N.; Kono, J.; Shaver, J.; Moore, V. C.; Hauge, R. H.; Smalley, R. E.; Wei, X. *Nano Lett.* **2004**, *4*, 2219–2221.
- (20) Casavant, M. J.; Walters, D. A.; Schmidt, J. J.; Smalley, R. E. *J. Appl. Phys.* **2003**, *93*, 2153–2156.
- (21) Walters, D. A.; Casavant, M. J.; Qin, X. C.; Huffman, C. B.; Boul, P. J.; Ericson, L. M.; Haroz, E. H.; O'Connell, M. J.; Smith, K.; Colbert, D. T.; Smalley, R. E. *Chem. Phys. Lett.* **2001**, *338*, 14–20.
- (22) Hone, J.; Llaguno, M. C.; Biercuk, M. J.; Johnson, A. T.; Batlogg, B.; Benes, Z.; Fischer, J. E. *Appl. Phys. A* **2002**, *74*, 339–345.
- (23) Pop, E.; Mann, D.; Wang, Q.; Goodson, K.; Dai, H. *Nano Lett.* **2006**, *6*, 96–100.
- (24) Girifalco, L. A.; Hodak, M.; Lee, R. S. *Phys. Rev. B* **2000**, *62*, 13104–13110.
- (25) Thess, A.; Lee, R.; Nikolaev, P.; Dai, H.; Petit, P.; Robert, J.; Xu, C.; Lee, Y. H.; Kim, S. G.; Rinzler, A. G.; Colbert, D. T.; Scuseria, G. E.; Tománek, D.; Fischer, J. E.; Smalley, R. E. *Science* **1996**, *273*, 483–487.
- (26) Bandow, S.; Rao, A. M.; Williams, K. A.; Thess, A.; Smalley, R. E.; Eklund, P. C. *J. Phys. Chem. B* **1997**, *101*, 8839–8842.
- (27) Ikeda, A.; Nobusawa, K.; Hamano, T.; Kikuchi, J.-i. *Org. Lett.* **2006**, *8*, 5489–5492.
- (28) Tasis, D.; Tagmatarchis, N.; Bianco, A.; Prato, M. *Chem. Rev.* **2006**, *106*, 1105–1136.
- (29) Matarredona, O.; Rhoads, H.; Li, Z.; Harwell, J. H.; Balzano, L.; Resasco, D. E. *J. Phys. Chem. B* **2003**, *107*, 13357–13367.
- (30) Islam, M. F.; Rojas, E.; Bergey, D. M.; Johnson, A. T.; Yodh, A. G. *Nano Lett.* **2003**, *3*, 269–273.
- (31) Arnold, M. S.; Green, A. A.; Hulvat, J. F.; Stupp, S. I.; Hersam, M. C. *Nat. Nanotechnol.* **2006**, *1*, 60–65.
- (32) Paloniemi, H.; Ääritalo, T.; Laiho, T.; Liu, H.; Kocharova, N.; Haapakka, K.; Terzi, F.; Seeber, R.; Lukkari, J. *J. Phys. Chem. B* **2005**, *109*, 8634–8642.
- (33) O'Connell, M. J.; Boul, P.; Ericson, L. M.; Huffman, C.; Wang, Y.; Haroz, E.; Kuper, C.; Tour, J.; Ausman, K. D.; Smalley, R. E. *Chem. Phys. Lett.* **2001**, *342*, 265–271.
- (34) Zorbas, V.; Ortiz-Acevedo, A.; Dalton, A. B.; Yoshida, M. M.; Dieckmann, G. R.; Draper, R. K.; Baughman, R. H.; Jose-Yacaman, M.; Musselman, I. H. *J. Am. Chem. Soc.* **2004**, *126*, 7222–7227.
- (35) Zheng, M.; Jagota, A.; Semke, E. D.; Diner, B. A.; McLean, R. S.; Lustig, S. R.; Richardson, R. E.; Tassi, N. G. *Nat. Mater.* **2003**, *2*, 338–342.
- (36) Zheng, M.; Jagota, A.; Strano, M. S.; Santos, A. P.; Barone, P.; Chou, S. G.; Diner, B. A.; Dresselhaus, M. S.; McLean, R. S.; Onoa, G. B.; Samsonidze, G. G.; Semke, E. D.; Usrey, M.; Walls, D. J. *Science* **2003**, *302*, 1545–1548.
- (37) Cathcart, H.; Nicolosi, V.; Hughes, J. M.; Blau, W. J.; Kelly, J. M.; Quinn, S. J.; Coleman, J. N. *J. Am. Chem. Soc.* **2008**, *130*, 12754–12744.
- (38) Minami, N.; Kim, Y.; Miyashita, K.; Kazaoui, S.; Nalini, B. *Appl. Phys. Lett.* **2006**, *88*, No. 093123–093126.
- (39) Numata, M.; Asai, M.; Kaneko, K.; Bae, A.-H.; Hasegawa, T.; Sakurai, K.; Shinkai, S. *J. Am. Chem. Soc.* **2005**, *127*, 5875–5884.
- (40) Star, A.; Stoddart, J. F.; Steuerman, D.; Diehl, M.; Boukai, A.; Wong, E. W.; Yang, X.; Chung, S.-W.; Choi, H.; Heath, J. R. *Angew. Chem., Int. Ed.* **2001**, *40*, 1721–1725.
- (41) Hwang, J.-Y.; Nish, A.; Doig, J.; Douven, S.; Chen, C.-W.; Chen, L.-C.; Nicholas, R. J. *J. Am. Chem. Soc.* **2008**, *130*, 3543–3553.
- (42) Chen, J.; Liu, H.; Weimer, W. A.; Halls, M. D.; Waldeck, D. H.; Walker, G. C. *J. Am. Chem. Soc.* **2002**, *124*, 9034–9035.
- (43) Kang, Y. K.; Lee, O.-S.; Deria, P.; Kim, S. H.; Park, T.-H.; Bonnell, D. A.; Saven, J. G.; Therien, M. J. *Nano Lett.* **2009**, *9*, 1414–1418.
- (44) Kang, Y. K.; Deria, P.; Carroll, P. J.; Therien, M. J. *Org. Lett.* **2008**, *10*, 1341–1344.
- (45) Castanet, A.-S.; Colobert, F.; Schlama, T. *Org. Lett.* **2000**, *2*, 3559–3561.
- (46) Oh, C. H.; Reddy, V. R. *Symlett* **2004**, *12*, 2091–2094.
- (47) Soderquist, J. A.; Matos, K.; Rane, A.; Ramos, J. *Tetrahedron Lett.* **1995**, *36*, 2401–2402.
- (48) Rubtsov, I. V.; Russo, R. M.; Albers, T.; Deria, P.; Luzzi, D. E.; Therien, M. J. *Appl. Phys. A* **2004**, *79*, 1747–1751.
- (49) Nelson, J. C.; Saven, J. G.; Moore, J. S.; Wolynes, P. G. *Science* **1997**, *277*, 1793–1796.
- (50) Lee, O.-S.; Saven, J. G. *J. Phys. Chem. B* **2004**, *108*, 11988–11994.
- (51) Bahr, J. L.; Mickelson, E. T.; Bronikowski, M. J.; Smalley, R. E.; Tour, J. M. *Chem. Commun.* **2001**, 193–194.
- (52) Starks, C. M.; Liotta, C. L.; Halpern, M. *Phase Transfer Catalysis*; Chapman & Hall: New York, 1994.
- (53) Weisman, R. B.; Bachilo, S. M. *Nano Lett.* **2003**, *3*, 1235–1238.
- (54) Choi, J. H.; Strano, M. S. *Appl. Phys. Lett.* **2007**, *90*, 223114–223116.
- (55) Jeng, E. S.; Moll, A. E.; Roy, A. C.; Gastala, J. B.; Strano, M. S. *Nano Lett.* **2006**, *6*, 371–375.
- (56) Yang, J.-P.; Kappes, M. M.; Hippel, H.; Unterreiner, A.-N. *Phys. Chem. Chem. Phys.* **2005**, *7*, 512–517.
- (57) Ando, T. *J. Phys. Soc. Jpn.* **2004**, *73*, 3351–3363.
- (58) Ma, Y.-Z.; Valkunas, L.; Bachilo, S. M.; Fleming, G. R. *J. Phys. Chem. B* **2005**, *109*, 15671–15674.
- (59) Klimov, V. I.; Mikhailovsky, A. A.; McBranch, D. W.; Leatherdale, C. A.; Bawendi, M. G. *Science* **2000**, *287*, 1011–1013.
- (60) Pedersen, T. G. *Phys. Rev. B* **2003**, *67*, No. 073401–073404.
- (61) Perebeinos, V.; Tersoff, J.; Avouris, P. *Phys. Rev. Lett.* **2004**, *92*, 257402–257404.